



Dynamic Analysis of Small Pig through Two and Three-Dimensional Liquid Pipeline

M. Lesani, M. Rafeeyan[†] and A. Sohankar

Department of Mechanical Engineering, Yazd University, Yazd, IRAN

[†]Corresponding Author Email: rafeeyan@yazduni.ac.ir

(Received March 18, 2010; Accepted September 13, 2009)

ABSTRACT

The derivation and solution of the two and three dimensional dynamic equations for a small pipeline inspection gauge (Pig) through a liquid pipeline is the main aim of this work. These equations can be used for synthesis of speed controller of a pig by using a bypass port in Pig. Momentum and energy equations are employed to study the influence of flow field on the Pig's trajectory. The pig is assumed to be a small rigid body with a bypass hole in its body. The variation of the diameter of the bypass port, which is controlled by a valve, is considered in this formulation. The path of the pig or geometry of the pipeline is assumed to be 2D and 3D curve. 2D and 3D simulations of the pig motion are performed individually and a case has been solved and discussed for each of them. The simulation results show that the derived equations are valid and effective for online estimating of the position, velocity and forces acting on the pig at any time of its motion.

Keywords: Pig, Dynamic equations, Liquid pipeline, Momentum and energy equations.

NOMENCLATURE

<p>D pipeline diameter g acceleration of gravity $f(x)$ function of the centerline of the pig in 2D $\text{sgn}(x)$ function of sign $F_{\mu} = \mu N$ dry friction force K_{SC}, K_{SE}, K_V coefficients of pressure losses L_{pig} length of the pig m mass of the pig N normal force acting on the pig p the fluid force acting on the pig in the pipeline direction</p>	<p>P_{tail} pressure in the tail of the pig P_{nose} pressure in the nose of the pig R radius of curvature of the pig's path s position variable along the pig's path V_{pig} velocity of the pig α constant value λ a time dependent parameter θ angle of the tangent to the centerline of the pipeline ρ density of fluid κ curvature</p>
--	---

1. INTRODUCTION

Pipelines are the safest method to transport fluids such as oil and gas products. After several years of the operation, the walls of pipelines suffer deterioration and pipeline conditions get worse. Passing the fluid through pipelines causes some types of corrosions on it. These corrosions can damage the pipeline and reduce its life, hydraulic efficiency, surface softness and so on. All types of pipeline defects increase costs of fluid transportation. For this reason, preventing the pipelines from these defects is always important for oil and gas industries. These damages of pipelines can be monitored only by pigs because there is no access for

observing the internal surface of the pipeline. Pigs are devices which are inserted into a pipeline and travels throughout it for inspection. A number of instruments such as MFL(magnetic flux leakage) sensors are carried by a smart pig to detect surface damages of the pipeline and their positions. The more knowledge about the dynamic behavior of the pigs, the more decrease in cost and time of the maintenance. Therefore, pipelines must be pigged regularly. Different kinds of pipe-wall defects that can be detected during pigging were explained by Hopkins (1992). Pigs must be run at constant speeds since the measuring process requires enough time for detecting damages. So, the study of

dynamic behavior of a pig is also necessary for its speed control.

The pig is usually driven by injected fluid flow behind its tail and expelled fluid flow in front of its nose. Thus, the dynamic behavior of the pig depends on the difference pressure across its body and height variations of its center of gravity. Determination of kinematics parameters of a pig and acting forces on it can be obtained by solving the governing equations of fluid flow together with the pig dynamic equations. Results of research on the motion of the pig in pipeline are scarcely found in the literatures. Most of results are commercially based on field experience. It seems that the first research in modeling of the pig motion has been introduced by McDonal et. al. (1946). The computation errors were generated in this work due to the used assumption and numerical approach. This modeling was modified and improved by removing some limitations by Barua (1982). The first pigging model was based on full two-phase transient flow formulation proposed by Kohda et. al. (1988). This model is composed of correlations for pressure drop across the pig, slug holdup, pigging efficiency, pig velocity model and a gas and liquid mass flow boundary condition applied to the slug front. Some other complementary researches for pigging simulation in two-phase flow straight pipelines were also reported by (Minami and Shoham 1991; Taitel et. al. 1989; Scoggins and M. W. 1977; Xiao-Xuan and Gong 2005). Transient pig motion through gas and liquid pipelines was presented by Nieckele et. al. (2001). Modeling and simulation for pig flow control in natural gas pipeline was studied by Nguyen et. al. (2001). One type of pig using bypass flow in natural gas pipeline was considered by some investigators such as Nguyen et. al. (2001). They proposed a simple nonlinear controller for controlling the pig velocity when it flows in natural gas straight pipeline.

In all the mentioned studies, researchers assumed that the pig moves in a straight line in the plane. Simulation of small pig in space pipeline was studied firstly by Saeidbakhsh et. al.(2009). This study was based on some simplifying assumptions such as: the pig is small, the pig/wall friction coefficient is constant and the driving force is time-dependent. In this research, the influence of the flow field is modeled only by time-dependent driving force acting on the pig. This assumption was made only for simplicity. In fact, solving coupled equations of pig motion and flow field can be a logic extension for further works.

The motivation for the present study is the obvious lack of information concerning to 2D and 3D dynamic analysis of a pig motion in the liquid pipelines. This extension is based on some simplifying assumptions: the pig is small, the pig/wall friction coefficient is constant and fluid is incompressible. The differential equations of the pig in the pipeline are derived by Newton's second law for pig and momentum and energy equations for fluid. The coupled equations are reduced to one equation with respect to parameter of curve technically. Finally, Rung-Kutta method is used for solving the derived equation. The 2D and 3D test cases are chosen to illustrate the application of this new formulation for these cases.

2. GOVERNING EQUATIONS OF THE PIG MOTION

2.1 Case 1: Two-Dimensional Path

Figure 1 shows a typical small pig moving inside a two dimensional pipeline and its free body diagram. In this figure, the mass of the pig, dry friction and normal force are denoted by m , $F_\mu = \mu N$, N respectively.

Also, the upstream acting forces on the pig due to fluid motion are shown by F_1 and F_2 , respectively, see Fig. 1. The dynamic equations of the pig derived from Newton's second law along the tangential and normal directions are as follows;

$$N - mg \cos \theta = ma_n \quad (1)$$

$$F_1 - F_2 - mg \sin \theta - \text{sgn}(\dot{x})F_\mu = ma_t \quad (2)$$

Where θ is the angle of the tangent to the centerline curve of the pipeline with respect to x -axis at any point; i.e. if $f(x)$ is assumed to be the function of the centerline of the pig, thus we can write

$$\theta = \tan^{-1} f'(x), \quad \cos \theta = \frac{1}{\sqrt{1 + f'(x)^2}} \quad (3)$$

If s is measured along the pig's path and the radius of curvature of the path is denoted by R , then the normal and tangential accelerations of the pig are as follows

$$V_{pig} = \dot{s} = \sqrt{1 + f'(x)^2} \dot{x} \quad (4)$$

$$a_n = \frac{V_{pig}^2}{R} = \frac{f''(x)}{\sqrt{1 + f'(x)^2}} \dot{x}^2 \quad (5)$$

$$a_t = \frac{d^2s}{dt^2} = \frac{f''(x)f'(x)}{\sqrt{1 + f'(x)^2}} \dot{x}^2 + \ddot{x} \sqrt{1 + f'(x)^2} \quad (6)$$

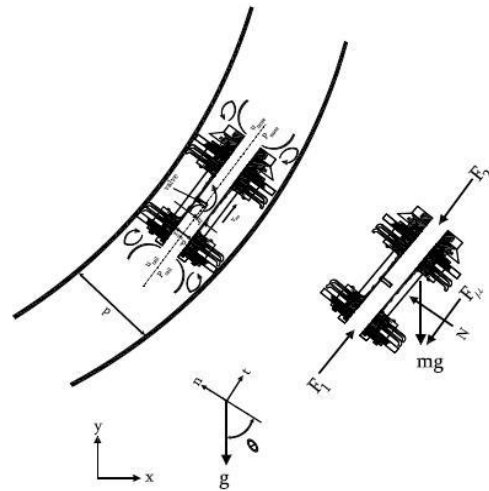


Fig. 1. Schematic view of a pig inside a planer pipeline

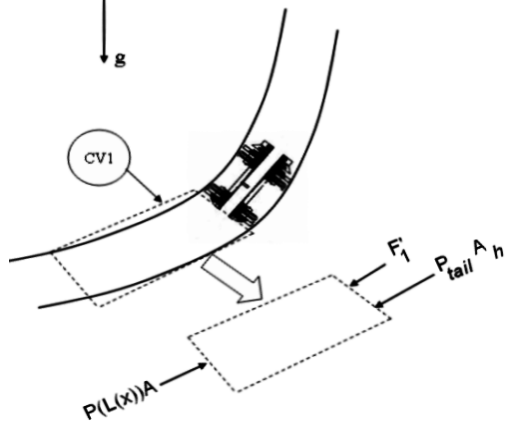


Fig. 2. The control volume No. 1.

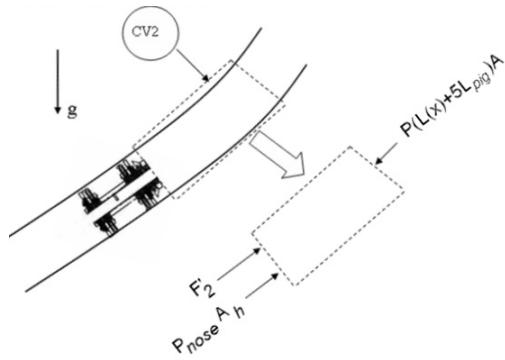


Fig. 3. The control volume No. 2.

To derive the term $F_1 - F_2$ in the left side of equation (2), one can combine the momentum and energy equations for fluid. To determine this term, the following assumptions are employed in this work.

1. The fluid inside the pipeline is incompressible.
2. The flow field is fully developed.
3. The coefficient of the friction between pig and pipeline is constant.
4. The coefficient of friction losses along the path is constant.

To determine the term $F_1 - F_2$, two control volumes are employed as shown in Figs. 2 and 3; one behind the pig and the other in front of it. Also it is assumed that the lengths of control volumes are the same and equals to $2L_{pig}$, where L_{pig} is the length of the pig.

The Eq. 7 shows the momentum equation for an inertial control volume.

$$\vec{F} = \vec{F}_S + \vec{F}_B = \int_{CS} \vec{V} \rho \vec{V} \cdot d\vec{A} + \frac{\partial}{\partial t} \int_{CV} \vec{V} \rho dV \quad (7)$$

In this equation, surface forces, body forces and velocity are denoted by \vec{F}_S , \vec{F}_B and V respectively. The different terms of the above equation in the

tangential direction (t -direction) for two control volumes are as follows:

$$F_{St1} = P(x)A - F'_1 - P_{tail}A_h, \quad \int_{CS1} V_i \rho \vec{V} \cdot d\vec{A} = \rho VA(V - V_h), \quad \frac{\partial}{\partial t} \int_{CV1} V_i \rho dV \approx 0 \quad (8)$$

$$F_{St2} = -P(x + 5L_{pig})A + F'_2 + P_{nose}A_h, \quad \int_{CS2} V_i \rho \vec{V} \cdot d\vec{A} = \rho VA(V_h - V), \quad \frac{\partial}{\partial t} \int_{CV2} V_i \rho dV \approx 0 \quad (9)$$

$$F_{Bt1} = F_{Bt2} = -2\rho g L_{pig} A \sin \theta = -2\rho g L_{pig} A \frac{f'(x)}{\sqrt{1 + f'(x)^2}} \quad (10)$$

where $P(x)$ is the pressure of the fluid on the pig, F'_1 and F'_2 are reactions of the pig on the control volumes ($F_1 = -F'_1$, $F_2 = -F'_2$), P_{tail} and P_{nose} are pressures of the fluid in behind and in front of the pig, A_h is the area cross section of the valve.

Pressure differences along the pipeline can be derived from the energy equation between two arbitrary positions as follows

$$\left(\frac{P_i}{\rho} + \alpha_i \frac{V_i^2}{2} + gZ_i \right) - \left[\frac{P(x)}{\rho} + \alpha(x) \frac{V(x)^2}{2} + gZ(x) \right] = h_{lf} \quad (11)$$

where α is an approximately constant value in the order of one in the turbulent flow, Z is the height of the selected position and V is the velocity of the fluid

and $h_{lf} = f \frac{x}{D} \frac{V^2}{2}$. Simplification of (11) gives

$$P(x) = P_i - f\rho \frac{L(x)}{D} \frac{V^2}{2} + \rho g [Z_i - Z(x)] \quad (12)$$

Substituting (8)-(10) and (12) in (7) for each control volumes, it leads to

$$F_1 - F_2 = (P_{tail} - P_{nose})A_h - \left[f\rho \frac{L(x + 5L_{pig}) - L(x)}{D} \frac{V^2}{2} + g\rho Z(x + 5L_{pig} \cos \theta) - \rho g Z(x) \right] A - 4\rho g A L_{pig} \frac{f'(x)}{\sqrt{1 + f'(x)^2}} \quad (13)$$

In general, the pressure difference between the tail and the nose of the bypass hole in the pig ($P_{tail} - P_{nose}$) is established from three parts; i.e. pressure losses from a sudden contraction at the tail (K_{SC}), valve inside the

hole (K_V) and a sudden expansion at the nose (K_{SE}).

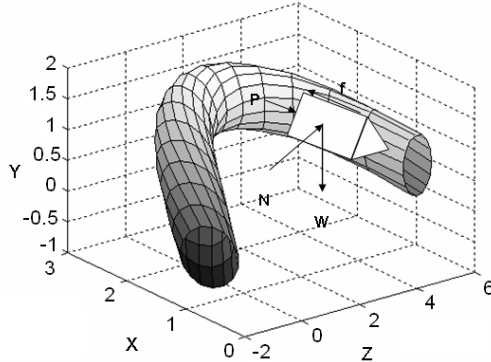


Fig. 4. Schematic view of a pig inside a 3D pipeline.

The following relations are suggested for the pressure difference and the losses coefficients in the fluid mechanics books and papers e.g. Nguyen et al. (2001).

$$P_{tail} - P_{nose} = \frac{K_{total} \rho (V_h - V_{pig})^2}{2} \quad (14)$$

where

$$K_{total} = K_{SC} + K_V + K_{SE}$$

$$K_{SC} = 0.42 \left(1 - \frac{d_{valve}^2}{d^2}\right)$$

$$K_{SE} = \left(1 - \frac{d_{valve}^2}{d^2}\right)^2, \quad K_V = f \left(\frac{h}{d_{valve}}\right)$$

$$\min(K_{total}) = \left(1 - \frac{d_{valve}^2}{d^2}\right) \left(1.42 - \frac{d_{valve}^2}{d^2}\right)$$

The normal force N is obtained if one substitutes Eqs. (3) and (5) in Eq. (1)

$$N = m \left[\frac{f''(x)}{\sqrt{1+f'(x)^2}} \dot{x}^2 + \frac{l}{\sqrt{1+f'(x)^2}} g \right] \quad (15)$$

The final equation of the pig can be derived by substituting all the terms in Eq. (2) as follows

$$\begin{aligned} & \frac{K_{total} \rho A^2 (V - \dot{x} \sqrt{1+f'(x)^2})^2}{2A_h} - f \rho \frac{5L_{pig}}{D} \frac{V^2}{2} \\ & + 4\rho g A L_{pig} \frac{f'(x)}{\sqrt{1+f'(x)^2}} - mg \frac{f'(x)}{\sqrt{1+f'(x)^2}} \\ & - \text{sgn}(\dot{x}) m \mu \left[\frac{f''(x)}{\sqrt{1+f'(x)^2}} \dot{x}^2 + \frac{g}{\sqrt{1+f'(x)^2}} \right] = \\ & m \left[\frac{f'(x)f''(x)}{\sqrt{1+f'(x)^2}} \dot{x}^2 + \ddot{x} \sqrt{1+f'(x)^2} \right] \end{aligned} \quad (16)$$

The equation is a second order ordinary differential equation that can be solved numerically.

2.2 Case 2: Three-Dimensional Path

Figure 4 shows the free body diagram of a typical small pig inside a three-dimensional pipeline. The weight of

the pig, dry friction force, normal force of the pipe wall and driving force are W , f , N , P , respectively. These forces, as shown in the Fig. 4, are three dimensional vectors in general. The position vector of the C.G. of the pig is denoted with $\mathbf{r}(\lambda)$ where λ is a time dependent parameter. We can write it with respect to its components, i.e.

$$\mathbf{r}(\lambda) = x(\lambda)\mathbf{i} + y(\lambda)\mathbf{j} + z(\lambda)\mathbf{k} \quad (17)$$

It is assumed that the gravitational force acts in the y -direction, then the weighting force of the pig is represented as $\mathbf{W} = -mg\mathbf{j}$. A frame of mutually orthogonal unit vectors is defined that it always travels along with a body moving in space (Thomas 1996). There are three vectors in the frame. One of them is the unit tangent vector $\boldsymbol{\tau}$. Another one is \mathbf{n} vector that gives the direction of $d\boldsymbol{\tau}/ds$. The third is $\mathbf{b} = \boldsymbol{\tau} \times \mathbf{n}$. These vectors and their derivatives are called as Serret-Frenet formulas (Sokolnikoff 1964), when available, give useful information about moving vehicles and paths they trace. The magnitude of the derivative $d\boldsymbol{\tau}/ds$ tells us how much a pig's path turns to the left or right as it moves along; it is called the curvature of the path. The number $|d\mathbf{b}/ds|$ tells us how much a pig's path rotates or twists as the pig moves along; it is called the torsion of the pig's path.

Although there are experimental data that indicate that the dynamic contact force (friction) might be a function of the pig velocity, however as Hopkins (1992), it is considered that it is independent of the pig velocity. This force acts in the direction of the pipe axis and in the opposite of the pig's motion. The direction of the normal force N is unknown; however it does not have any component in the tangential direction of the pig's path. The driving force P acts in the direction of the pipe axis. This force depends on the pressure difference between the nose and the tail of the pig and other variables in a complex problem.

The dynamic equations of the pig derived from the Newton's Second Law along \mathbf{n} , $\boldsymbol{\tau}$ and \mathbf{b} directions are as follow;

$$p(\lambda) - \text{sgn}(V)f + mg\boldsymbol{\tau} = m \frac{d^2s}{dt^2} \quad (18)$$

$$N_1 + mg_n = mV^2/R \quad (19)$$

$$N_2 + mg_b = 0 \quad (20)$$

where,

$$N = N_1\mathbf{n} + N_2\mathbf{b}, \quad \mathbf{W} = mg\boldsymbol{\tau} + mg_n\mathbf{n} + mg_b\mathbf{b}$$

and s is measured along the pig's path. If we use the chain rule and differentiate from Eq. (17) for obtaining

the \mathbf{n} , $\boldsymbol{\tau}$ and \mathbf{b} at all points and denote $d/dt = (\dot{\quad})$ and $d/d\lambda = (\prime)$, then the following relation will be obtained;

$$\boldsymbol{\tau} = \frac{x'\mathbf{i} + y'\mathbf{j} + z'\mathbf{k}}{\sqrt{x'^2 + y'^2 + z'^2}} \quad (21)$$

Based on the first Serret-Frenet formula, we have, $d\boldsymbol{\tau}/ds = \kappa \mathbf{n}$ where κ is the curvature and will be determined from;

$$\frac{d\boldsymbol{\tau}}{ds} = \frac{d\boldsymbol{\tau}}{dt} \cdot \frac{dt}{ds} = a_1 \mathbf{i} + a_2 \mathbf{j} + a_3 \mathbf{k}$$

$$a_1 = \frac{(x''y'^2 + z'^2x'' - x'y'y'' - x'z'z'')}{\Delta}$$

$$a_2 = \frac{(x'^2y'' + y''z'^2 - y'x'x'' - y'z'z'')}{\Delta}$$

$$a_3 = \frac{(y'^2z'' + x'^2z'' - z'x'x'' - z'y'y'')}{\Delta}$$

$$\Delta = x'^2 + y'^2 + z'^2 \quad (22)$$

$$\kappa = \frac{1}{R} = \left| \frac{d\boldsymbol{\tau}}{ds} \right| = \sqrt{a_1^2 + a_2^2 + a_3^2} \quad (23)$$

Also the normal unit vector \mathbf{n} can be obtained from Eqs. (22), i.e.

$$\mathbf{n} = (a_1 \mathbf{i} + a_2 \mathbf{j} + a_3 \mathbf{k}) / \Delta \quad (24)$$

The second normal unit vector is derived from the outer cross product of $\boldsymbol{\tau}$ and \mathbf{n} , i.e.

$$\mathbf{b} = \boldsymbol{\tau} \times \mathbf{n} = \frac{1}{\sqrt{\Delta(a_1^2 + a_2^2 + a_3^2)}} [(a_3y' - a_2z')\mathbf{i} - (a_3x' - a_1z')\mathbf{j} + (a_2x' - a_1y')\mathbf{k}] \quad (25)$$

Since the projection of the vector V_1 on V_2 is equal to $V_1 \cdot V_2 / |V_2|$ then g_n, g_t and g_b can be obtained as:

$$g_n = -\frac{ga_2}{\sqrt{a_1^2 + a_2^2 + a_3^2}} \quad (26)$$

$$g_b = \frac{g(a_3x' - a_1z')}{\sqrt{\Delta(a_1^2 + a_2^2 + a_3^2)}} \quad (27)$$

$$g_t = -\frac{gy'}{\sqrt{x'^2 + y'^2 + z'^2}} \quad (28)$$

Now, one needs to calculate the remaining unknown terms in Eqs. (18) to (20) i.e.,

$$\mathbf{V} = \dot{\mathbf{r}}(\lambda) = (x'\mathbf{i} + y'\mathbf{j} + z'\mathbf{k})\dot{\lambda} \quad (29)$$

If one substitutes Eqs. (25) and (26) and the magnitude of Eq.(29) in Eqs. (19) and (20), the components of normal forces are determined as:

$$N_1 = m[\dot{\lambda}\Delta\sqrt{a_1^2 + a_2^2 + a_3^2} + \frac{ga_2}{\sqrt{a_1^2 + a_2^2 + a_3^2}}] \quad (30)$$

$$N_2 = -\frac{mg(a_3x' - a_1z')}{\sqrt{\Delta(a_1^2 + a_2^2 + a_3^2)}} \quad (31)$$

$$|\mathbf{N}| = \sqrt{N_1^2 + N_2^2}, \quad f = \mu|\mathbf{N}| \quad (32)$$

Finally, substituting Eqs. (32) and (29) in Eq. (18) results in:

$$p(\lambda) - \text{sgn}(V)\mu m h_1 - \frac{mgy'}{\sqrt{\Delta}} = \frac{m}{\sqrt{\Delta}} \{x'(x''\dot{\lambda}^2 + \ddot{\lambda}x') + y'(y''\dot{\lambda}^2 + \ddot{\lambda}y') + z'(z''\dot{\lambda}^2 + \ddot{\lambda}z')\} \quad (33)$$

where

$$h_1 = \{(\Delta\sqrt{a_1^2 + a_2^2 + a_3^2} + \frac{ga_2}{\sqrt{a_1^2 + a_2^2 + a_3^2}})^2 + (\frac{g(a_3x' - a_1z')}{\sqrt{\Delta(a_1^2 + a_2^2 + a_3^2)}})^2\}^{0.5}$$

The term $p(\lambda)$ can be obtained from momentum and energy equations in pipeline direction as follows

$$p(\lambda) = \frac{K_{total} A^2 \rho [V - \dot{\lambda}\sqrt{(x'^2 + y'^2 + z'^2)}]^2}{2A_h} - f\rho \frac{5L_{pig}}{D} \frac{V^2}{2} A + \frac{4\rho gAL_{pig}\dot{\lambda}y'}{|\dot{\lambda}|\sqrt{x'^2 + y'^2 + z'^2}} \quad (34)$$

Substituting Eq. (34) in Eq. (33) and rearranging it with respect to $\dot{\lambda}$ results in the final differential equation as

$$\ddot{\lambda} = \frac{|\dot{\lambda}|}{\dot{\lambda}} h_2 \left\{ \left[\dot{\lambda}^2 (x'^2 + y'^2 + z'^2) \sqrt{a_1^2 + a_2^2 + a_3^2} \right] + \frac{ga_2}{\sqrt{(x'^2 + y'^2 + z'^2)} \sqrt{a_1^2 + a_2^2 + a_3^2}} \right\} + \left\{ \left[\frac{|\dot{\lambda}|}{\dot{\lambda}} \frac{g(a_3x' - a_1z')}{\sqrt{(x'^2 + y'^2 + z'^2)} \sqrt{a_1^2 + a_2^2 + a_3^2}} \right]^2 \right\}^{0.5} + \frac{gy' - \dot{\lambda}^2 (x'x'' + y'y'' + z'z'')}{(x'^2 + y'^2 + z'^2)} \quad (35)$$

where

$$h_2 = \frac{1}{\sqrt{x'^2 + y'^2 + z'^2}} \left[\frac{K_{total} \rho A^2 V}{2mA_h} - \frac{K_{total} \rho A^2 \dot{\lambda} \sqrt{x'^2 + y'^2 + z'^2}}{2mA_h} + f\rho \frac{5L_{pig}}{D} \frac{V^2}{2m} A - 4\rho gAL_{pig} \frac{\dot{\lambda}y'}{m\sqrt{\dot{\lambda}^2 (x'^2 + y'^2 + z'^2)}} - \text{sgn}(\dot{\lambda}\sqrt{x'^2 + y'^2 + z'^2})\mu \right]$$

The above equation is a nonlinear differential equation with respect to λ , which can be solved by a numerical technique such as Runge-Kutta based on initial conditions. When parameter $\dot{\lambda}$ is determined in each time instant t , then the position and the velocity of the pig can be calculated.

3. NUMERICAL STUDIES

In order to show the validity of the developed equations, three case studies were designed and solved by the proposed numerical technique.

3.1 Case 1

For the first case study, let us assume a 2D pipeline with the curve equation as $y(x) = 0.5(x + \sin x)$. Figure 5 shows the pipeline curve. The numerical values for the mass of the pig, length of the pig, pipe diameter and the bypass diameter are assumed to be 50 kg, 0.3 m, 0.25 m and 0.12 m, respectively.

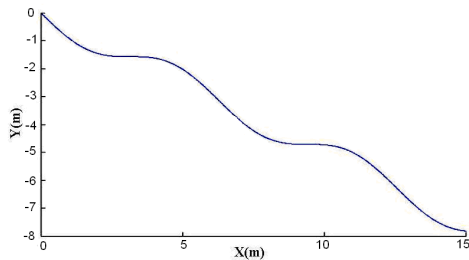


Fig. 5. The pipeline curve in 2D for case study 1.

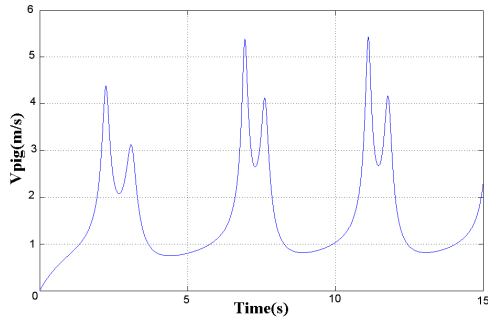


Fig. 6. Velocity of the pig for case study 1.

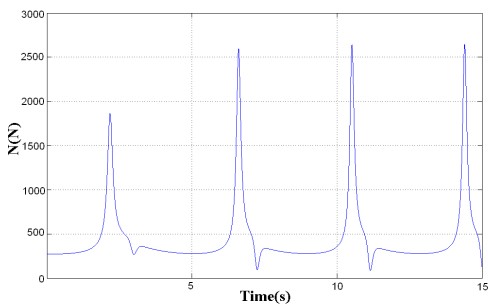


Fig. 7. Normal force exerted on the pig for case study 1.

The fluid is water with density of 1000 kg/m^3 and velocity of 5 m/s . The inlet pressure of the pipeline is 8 bars. The dynamic and static coefficients of friction are assumed to be 0.2 and 0.3, respectively. The pig position at initial time is at the point $x(0) = y(0) = 0$.

The aim of this example is to test the validation of the formulations for the simpler case, i.e. two-dimensional path. The geometric curvilinear periodic nature of this

pipeline can help this examination. Figure 6 shows the velocity of the pig with respect to time. This figure shows the periodic variations of the pig's velocity. Figure 7 also shows the periodic nature of the normal force acting on the pig.

3.2 Case 2

The geometry of the selected pipeline for the second case is shown in Fig. 8. It is similar to a well known space curve such as helix with the following parametric equations

$$x(\lambda) = 6 \sin \lambda, \quad y(\lambda) = 6 \cos \lambda, \quad z(\lambda) = 6 \lambda$$

The fluid is water with $\rho = 1000 \text{ kg/m}^3$ and its velocity in the pipeline is 20 m/s . The mass of the pig is 50 kg and static and dynamic friction coefficients are 0.3 and 0.2, respectively. The pig moves from origin at $t=0$ and its motion is recorded up to 15 seconds.

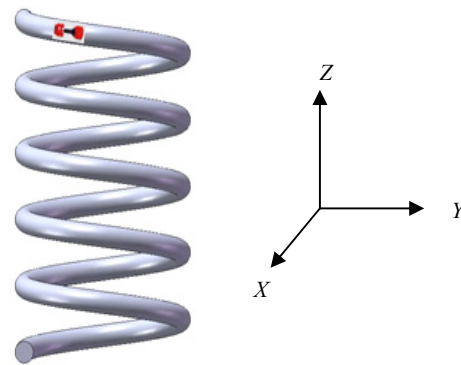
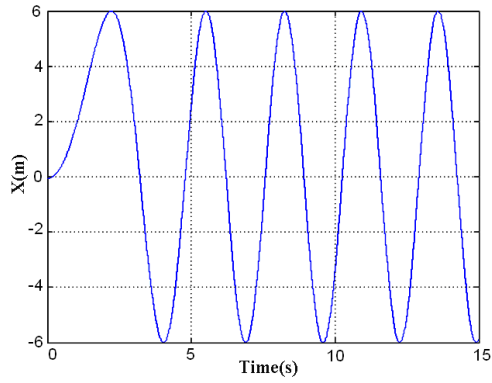


Fig. 8. A helix-type pipeline.

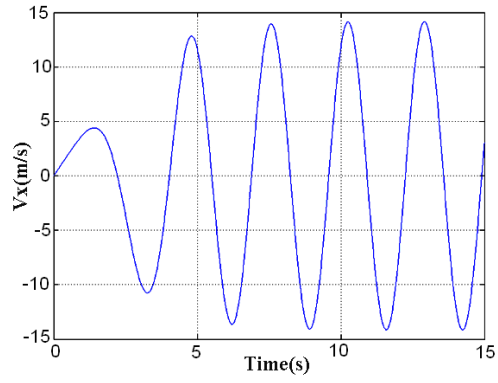
This example shows the validation of the above formulation for three dimensional path, where its geometric is curvilinear periodic nature. Figures 9a to 9f show the position and velocities of the pig in the x, y and z-directions with respect to time. The positions of the pig in the x and y-directions have a periodic nature. The velocities in these directions have the same sorts of trends. However, the velocity of the pig starts from zero and decreases down to a certain level and then remains constant. It takes about 5 seconds. This is true because of the special geometry of the pipeline. Since there is no difference between any two points of the path and also the area of hole is constant, the pig's velocity reaches a constant value. These results validate the modeling and formulation of the present research. Also, these results are very similar to the case 1 of Saeidbakhsh et al.(2009) qualitatively. Comparison between these results shows that the fluid decreases the motion of the pig in the pipeline because in this research, effects of the fluid are included in equations.

3.3 Case 3

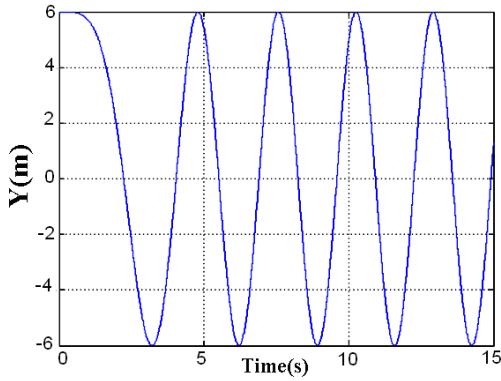
The geometry of the selected pipeline for the third test case is shown in Fig. 10. The parametric equations of this path are



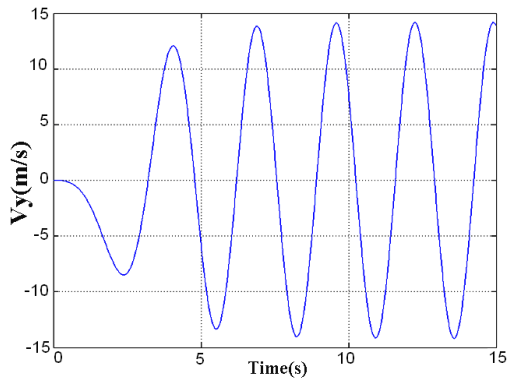
a) Position of the pig in x direction



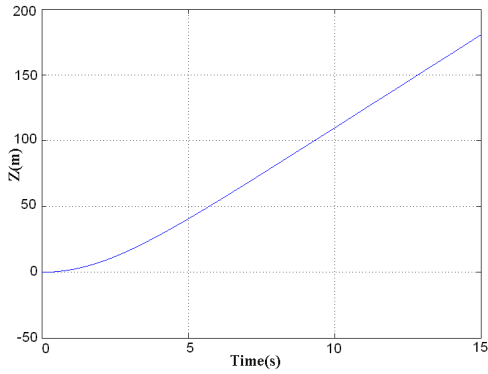
b) Velocity of the pig in x direction



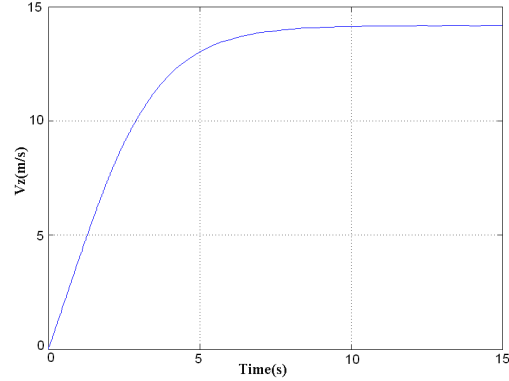
c) Position of the pig in y direction



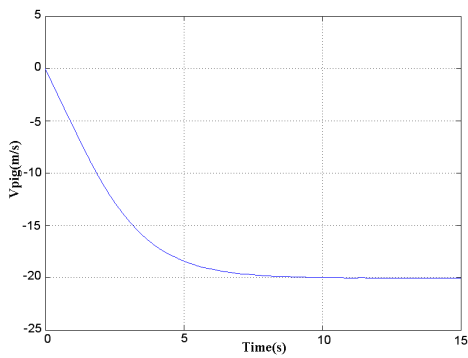
d) Velocity of the pig in y direction



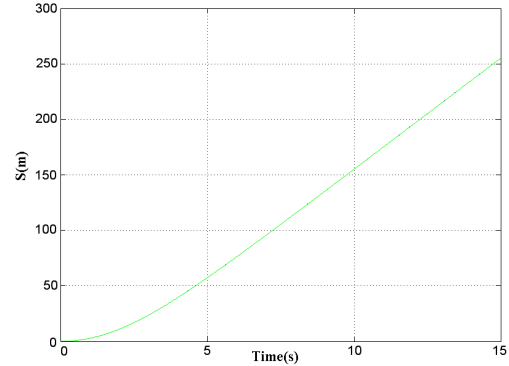
e) Position of the pig in z direction



f) Velocity of the pig in z direction



g) Velocity of the pig in tangential direction



h) Distance from inlet of the pipe

Fig. 9. Simulation results of helix-type pipeline.

this case also are in agreement with the physical nature of the problem.

The third case, which is a space pipeline whose geometry is arbitrary, also validated the proposed procedure for this case.

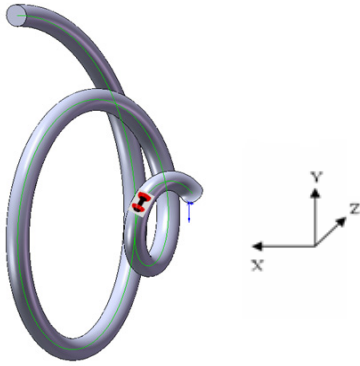


Fig. 10. Selected geometry of pipeline for the case 3.

$$x = \lambda^2 \quad y = \lambda^2 \sin \lambda \quad z = \lambda^2 \cos \lambda$$

The fluid is water with $\rho = 1000 \text{ kg/m}^3$ and its velocity in the pipeline is 5 m/s . The mass of the pig is 50 kg and static and dynamic friction coefficients are 0.3 and 0.2 , respectively. The pig does not move from origin at $t=0$ and its motion is recorded up to 15 seconds.

The results are shown in Fig. 11. The geometry of the pipeline for this test case is arbitrary. The Runge-kutta method with a sampling time of 0.01 s was used for this case study. All figures show that the pig stops after 12 seconds, where the equilibrium conditions establish for pig in the pipeline at this moment. In this case, the direction of friction force and also its type (static or dynamic) varies in some times of motion. Also, the gravity force of the pig and the fluid driving force frequently vary. Then, as Fig. 11g shows, the pig velocity reaches to zero in some times and accelerates again. This example shows the ability of the formulation for pigging estimation. The best pig can be select for a special pipeline based on the formulation in this research. Also, sticking of a pig in a special pipeline can be estimated by this formulation.

4. CONCLUSION

A numerical method for dynamic analysis of a pig in the space curves was presented in this work. The differential equations of the pig in the pipeline were derived by Newton's second law for pig, momentum and energy equations for fluid in the pipelines (Serret-Frenet formula for dynamic analysis of pigs in space curves). This method is limited by the incompressible fluid flow in the pipeline.

Three numerical case studies were selected to validate the proposed procedure of this paper. Results from the first case which is a 2D example, are in agreement with the physical nature of the problem.

The second case study is also a pipeline whose special geometry (helix type) helps someone to check the validation of the proposed procedure. The results from

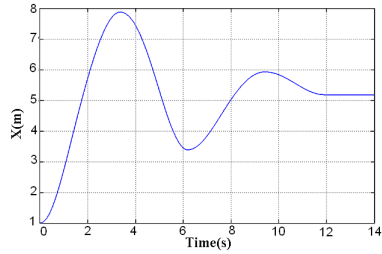
REFERENCES

- Barus, S. (1982). *An Experimental Verification and Modification of The McDonald and Baker Pigging Model For Horizontal Flow*, Ph.D Thesis, University of Tulsa, Texas, USA.
- Hopkins, P. (1992). *The Assessment of Pipeline Defects During Pigging Operations*, in *Pipeline Pigging Technology*. Tiratsoo J.N.H.(ed.), Gulf Professional Publishing, 2nd ed., pp. 303-324.
- Kohda, K., Y. Suzukawa, and H. Furukwa (1988). *A new method for analyzing transient flow after pigging scores well*. *Oil and Gas Journal* 9(May), 40-47.
- McDonal A. and O. Baker (1964). *Multiphase flow in (Gas) pipelines*, *Oil and Gas Journal* 62(24):68-71, 62(25):171-175, 62(26):64-67, 62(27): 118-119.
- Minami, K. and O. Shoham (1991). *Pigging dynamics in two-phase flow pipelines: experiment and modeling*, *SPE Prod. Facil.*, 10(4), 225-231.
- Nguyen T.T., S.B. Kim, H.R. Yoo, and Y.W. Rho (2001). *Modeling and simulation for pig flow control in natural gas pipeline*, *KSME Int. J.* 15(8), 1165-1173.
- Nguyen T.T, H.R. Yoo , Y.W. Rho, and S.B. Kim (2001, June). *Speed control of pig bypass flow in natural gas pipeline*, *International Symposium on Industrial Electronics*, Pusan, Korea.
- Nieckele A.O., A.M.B Braga, L.F.A. Azevedo (2001). *Transient pig motion trough gas and liquid pipelines*, *Journal of Energy Resources. ASME* 123, 260-269.
- Saeidbakhsh M., M. Rafeeyan, S. Ziaei-rad (2009) *Dynamic analysis of small pigs in space pipelines*, *Oil and Gas Science and Technology*. 64(2), 155-164.
- Scoggins, Jr. (1977). *Numerical simulation model for transient two-phase flow in a pipeline*, PhD Thesis, University of Tulsa, Texas, USA.
- Sokolnikoff, I.S. (1964). *Tensor Analysis*, New York, USA, John Wiley and Sons.

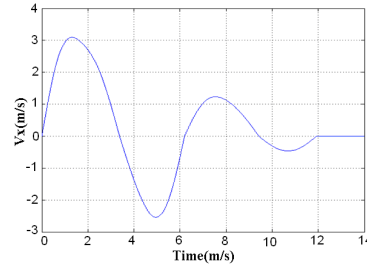
Taitel, Y., O. Shoham, and J.P. Brill (1989). Simplified transient solution and simulation of two-phase flow in pipelines, *Chem. Eng. Sci.* **44**, 1353-1359.

Xiao-Xuan X., and J. Gong (2005). Pigging simulation for horizontal gas-condensate pipelines with low-liquid loading, *Journal of Petroleum Science Engineering.* **48**, 272-280.

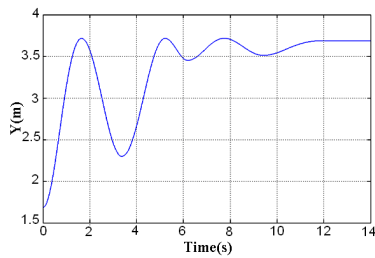
Thomas G.B. and R.L. Finney (1996). *Calculus and Analytic Geometry*, USA, Addison-Wesley Publishing Company(9th edition).



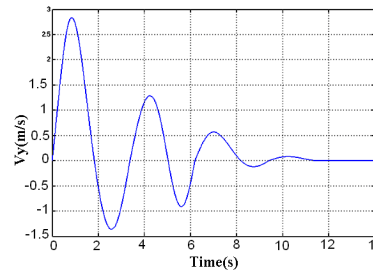
a) Position of the pig in x direction.



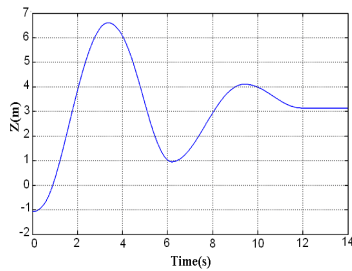
b) Velocity of the pig in x direction.



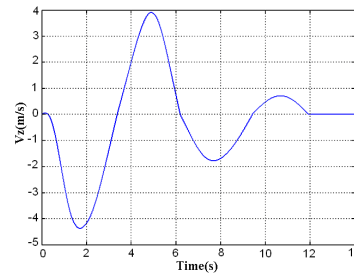
c) Position of the pig in y direction.



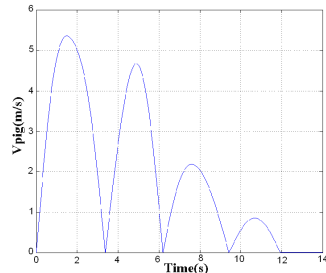
d) Velocity of the pig in y direction.



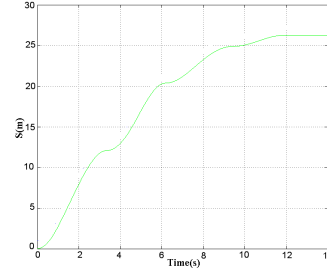
e) Position of the pig in z direction.



f) Velocity of the pig in z direction.



g) Velocity of the pig in tangential direction.



h) Distance from inlet of the pipe.

Fig. 11. Simulation results of the pipeline of the test case 3.